

# 1 Differentiating between crop and soil effects on soil moisture 2 dynamics

3 Helen Scholz<sup>1</sup>, Gunnar Lischeid<sup>2,3</sup>, Lars Ribbe<sup>1</sup>, Ixchel Hernandez Ochoa<sup>4</sup>, Kathrin Grahmann<sup>2</sup>

4 <sup>1</sup>Institute for Technology and Resources Management in the Tropics and Subtropics (ITT), TH Köln, Cologne, Germany

5 <sup>2</sup>Leibniz Centre for Agricultural Landscape Research (ZALF), Müncheberg, Germany

6 <sup>3</sup>Institute for Environmental Sciences and Geography, University of Potsdam, Potsdam, Germany

7 <sup>4</sup>Institute of Crop Science and Resource Conservation (INRES), Crop Science Group, University of Bonn, Bonn, Germany

8 *Correspondence to:* kathrin.grahmann@zalf.de

9 **Abstract.** There is urgent need to develop sustainable agricultural land use schemes. Intensive crop production has induced  
10 increased greenhouse gas emissions and enhanced nutrient and pesticide leaching to groundwater and streams. Climate change  
11 is also expected to increase drought risk as well as the frequency of extreme precipitation events in many regions.  
12 Consequently, sustainable management schemes require sound knowledge of site-specific soil water processes that explicitly  
13 take into account the interplay between soil heterogeneities and crops. In this study, we applied a principal component analysis  
14 to a set of 64 soil moisture time series from a diversified cropping field featuring seven distinct crops and two weeding  
15 management strategies.

16 Results showed that about 97% of the spatial and temporal variance of the data set was explained by the first five principal  
17 components. Meteorological drivers accounted for 72.3% of the variance, 17.0% was attributed to different seasonal behaviour  
18 of different crops. While the third (4.1%) and fourth (2.2%) principal component were interpreted as effects of soil texture and  
19 cropping schemes on soil moisture variance, respectively, the effect of soil depth was represented by the fifth component  
20 (1.7%). However, neither topography nor weed control had a significant effect on soil moisture variance. Contrary to common  
21 expectations, soil and rooting pattern heterogeneity seemed not to play a major role. Findings of this study highly depend on  
22 local conditions. However, we consider the presented approach generally applicable to a large range of site conditions.

## 23 1 Introduction

24 Agriculture plays a major role to ensure the provision of food to a growing global population. At the same time, climate change  
25 is putting yield stability at risk due to extreme weather events, rising the need for sustainable management of resources, such  
26 as water and soil (Trnka et al., 2014). The transformation from large homogeneously cropped fields towards diversified  
27 agricultural landscapes has been identified as an opportunity that can contribute to climate adaptation due to the positive effects  
28 on multiple ecosystem services (Tamburini et al., 2020), and cropping system resilience to climatic extremes (Birtal and  
29 Hazrana, 2019). Additionally, crop diversification is highly beneficial by reducing soil erosion through permanent soil cover  
30 (Paroda et al., 2015), and by improving resource use efficiency through wider crop rotations (Rodriguez et al., 2021).

31 In terms of soil water dynamics, crop and management diversification can lead to improved water-stable macro-aggregation,  
32 reduced soil compaction and increased soil organic carbon, which can reduce soil water infiltration and improve water retention  
33 (Alhameid et al., 2020; Fischer et al., 2014; Karlen et al., 2006; Koudahe et al., 2022; Nunes et al., 2018). Korres et al. (2015)  
34 reported that spatial variability of soil moisture was mainly driven by soil characteristics, followed by crop cover and  
35 management. Soil moisture is also affected by soil texture and pore size distribution (Krauss et al., 2010; Rossini et al., 2021;  
36 Pan and Peters-Lidard, 2008). The quantification of the impact of these effects on soil moisture variability is important, for  
37 instance for hydrological applications and adopted management practices in agriculture (Hupet and Vanclouster, 2002).  
38 As the diversity of independent variables in agricultural systems increases, demands for frequency and spacing of soil moisture  
39 measurements and related data interpretation grow. Therefore, soil sensor networks are receiving increased attention,  
40 particularly in Precision Agriculture (PA; Bogen et al., 2022; Salam and Raza, 2020), where the main goal is to increase  
41 efficiency and productivity at the farm level while minimizing the negative impacts on the environment (Taylor and Whelan,  
42 2010). Soil sensor networks can meaningfully contribute to PA as they can be used for various purposes, including the  
43 delineation of management zones (Khan et al., 2020; Salam and Raza, 2020). Still, one of the most important demands to be  
44 fulfilled by soil sensor networks is soil moisture monitoring, as accurate measurement of soil water content can play an  
45 important role in improving water management and therefore, crop yields (Salam, 2020).  
46 Wireless solutions, for instance based on LoRaWAN (Long Range Wide Area Network) technology, in combination with  
47 electromagnetic soil moisture sensors avoid labour-intensive and destructive soil moisture measurements that disrupt field  
48 traffic. The development of such wireless sensor networks (WSN) enables broad and affordable application also in areas with  
49 low cellular coverage (Cardell-Oliver et al., 2019; Lloret et al., 2021; Placidi et al., 2021; Prakosa et al., 2021).  
50 The evolution of WSN does not only have benefits for management but is also of high relevance for fostering the  
51 understanding of hydrological dynamics in the vadose zone. High-resolution datasets measured under real farming conditions  
52 can be used to characterize and analyse spatio-temporal dynamics of soil water. Due to the large size of data sets that are  
53 recorded with WSN, sophisticated data analysis approaches are required to detect hidden patterns and determine influence  
54 factors on soil moisture variability (Vereecken et al., 2014). With the introduction of multiple-points geostatistics, it became  
55 possible to not only analyse patterns but also connect them with factors affecting soil moisture, such as topography, texture,  
56 crop growth and water uptake, and land management (Brocca et al., 2010; Strebelle et al., 2003). Wavelet analysis can analyse  
57 both localized features as well as spatial trends through which non-stationary variation of soil properties can be considered (Si,  
58 2008). Cross-correlation analysis allowed linking soil moisture variability to climatic variables (Mahmood et al., 2012).  
59 Furthermore, temporal stability analyses detect spots in the investigated area which are consistently wetter or drier than the  
60 mean soil moisture (Baroni et al., 2013; Vachaud et al., 1985; Vanderlinden et al., 2012). This method was already successfully  
61 used to detect soil moisture patterns related to soil properties, vegetation, and topography (Zhao et al., 2010).  
62 Principal component analysis (PCA) is another method that was successfully applied for soil moisture variability analysis at  
63 the field (Hohenbrink et al., 2016; Hohenbrink and Lischeid, 2015; Martini et al., 2017), catchment (Korres et al., 2010;  
64 Lischeid et al., 2017; Nied et al., 2013; Graf et al., 2014), and regional (Joshi and Mohanty, 2010) scale. These studies build

65 on previous applications in climatology where the term “Empirical Orthogonal Functions” is used (Bretherton et al., 1992) and  
66 are examples for how space and time dimensions can be disentangled and assigned to influencing factors. Additionally, the  
67 propagation of hydrological signals (e.g. precipitation events) over depth can be assessed (Hohenbrink et al., 2016). This opens  
68 up great opportunities to improve the knowledge of changing soil water dynamics in complex diversified agricultural systems  
69 with increasing heterogeneity (e. g. soil texture) and site-specific adjustment of crop and field management which, to our  
70 knowledge, have hardly been studied so far. The main objective of this study was to identify the drivers of soil moisture  
71 variability in a diversified cropping field in terms of soil texture, crop selection and field management by applying PCA.  
72 Special focus was put on the interpretation of spatial and temporal effects of crop diversification and of soil heterogeneities on  
73 soil moisture dynamics. For this, we analysed a high-resolution soil moisture data set measured by a novel underground  
74 LoRaWAN monitoring system with soil moisture sensors in different depths of the vadose zone at a spatial-temporally  
75 diversified agricultural field in Northeast Germany. The novelty of this WSN relies on its unique on-farm installation  
76 environment. The deployment of transmission units in 0.3 m soil depth and 180 sensors in up to 0.9 m soil depth allows high  
77 spatio-temporal resolution wireless data transmission, and enables conventional farming practices like machinery traffic,  
78 tillage and mechanical weeding.

## 79 **2 Materials and methods**

### 80 **2.1 Study site**

81 The study site (52°26'51.8"N 14°08'37.7"E, 66-83 m.a.s.l.) is located near the city of Müncheberg in the federal state of  
82 Brandenburg in Northeastern Germany. The landscape is classified as a hummocky ground moraine that formed during the  
83 last glacial periods. Glacial and interglacial processes as well as subsequent erosion resulted in highly heterogeneous soils  
84 (Deumlich et al., 2018), being classified as Dystric Podzoluvisols according to the FAO scheme (Fischer et al., 2008). In the  
85 top 0.3 m soil layer, total organic carbon was 0.94% and total nitrogen content was 0.07%, and pH was 6.12. Between January  
86 1991 and December 2020, the mean annual temperature in Müncheberg was 9.6°C, and the mean annual sum of precipitation  
87 was 509 mm (DWD Climate Data Center (CDC), 2021).

### 88 **2.2 Experimental setup**

89 The data collection was carried out from December 2020 until mid of August 2021 in the patchCROP experiment (Grahmann  
90 et al, 2024; Donat et al., 2022). This landscape experiment has been set up to study the multiple effects of cropping system  
91 diversification on productivity, crop health, soil quality, and biodiversity. To that end, a cluster analysis was carried out based  
92 on soil maps and multi-year (2010 to 2019) yield data to identify high and low yield potential zones in the 70-ha large field  
93 (Donat et al., 2022). Afterwards, single experimental units comprising 30 patches with an individual size of 0.52 ha (72 m ×  
94 72 m) each, have been implemented in both, high and low yield potential zones where each of those zones is characterized by  
95 varying soil conditions and a site-specific five-year, legume-based crop rotation (Grahmann et al., 2024). The remaining area

96 outside of the 30 patches was planted with winter rye. For the current study, twelve out of 30 patches were considered (Table  
97 1, Figure 1). Specific patches were selected to capture the soil heterogeneities in terms of soil texture, but also the seasonal  
98 patterns of the crop rotation that may have important effects on the soil water dynamics such as crop types, presence of cover  
99 crops or fallow periods. In the cropping season 2020/2021, seven different main crops were grown. For subsequent data  
100 interpretation, crops have been grouped into A) winter crops, B) fallow, followed by summer crops and C) cover crops,  
101 followed by summer crops. In seven out of twelve considered patches, weed control was carried out with herbicide application,  
102 referred as “conventional” pesticide application, while in the remaining five patches, “reduced” pesticide management was  
103 carried out by mainly using mechanical weeding, by harrowing, blind harrowing, and hoeing. Only in the case of high weed  
104 pressure herbicides were applied. Due to the potential impact of mechanical weeding, i.e., on rainwater infiltration, soil  
105 evaporation and topsoil rooting intensity, we differentiate between these modes of weed control.

## 106 **2.3 Data collection**

### 107 **2.3.1 Soil moisture data**

108 Soil moisture was recorded by a long-range-wide-area network (LoRaWAN) based WSN. In each patch, one Dribox box  
109 equipped with a SDI-12 distributor (serial data interface at 1200 baud rate, TBS04, TekBox, Saigon, Vietnam) connected to  
110 six TDR-sensors (TDR310H, Acclima, Meridian, USA) and attached to an outdoor remote terminal unit (RTU) fully  
111 LoRaWAN compliant (TBS12B: 4+1 channel analogue to SDI-12 interface for 24 Bit A/D conversion of sensor signals,  
112 TekBox, Saigon, Vietnam) was installed as LoRa node. It was deployed at least 0.3 m below ground to allow field traffic and  
113 soil tillage. The sensors and boxes were installed between August and November 2020. At two georeferenced locations within  
114 each patch, soil moisture sensors were installed in 0.3, 0.6 and 0.9 m depth, respectively. Sensors were approximately 2 m  
115 apart from the LoRa node in angles between 45° and 60° (Figure 1). Soil moisture sensors at 0.3 m were placed horizontally,  
116 while sensors at 0.6 and 0.9 m depth were placed vertically using auger-made boreholes and extension tubes for soil insertion.  
117 Communication of LoRa nodes was wireless and autarkic in energy supply. Thus, no electric cabling except from connections  
118 between sensors and LoRa nodes was needed. Under optimum conditions, battery running time of the LoRa nodes can be up  
119 to 12 months but can be reduced to 8 months when radio transmission is attenuated (e.g. due to near water-saturated soil)  
120 which then increases power consumption (Bogena et al., 2009). Data was recorded every 20 minutes by the LoRa nodes  
121 through a LoRa-WAN Gateway DLOS8 (UP GmbH, Ibbenbüren, Germany) which was equipped with the modem TL-  
122 WA7510N (TP Link, Hong Kong, China) to transfer the data to a cloud from where collected data could be accessed directly  
123 after the measurement. The time series included in this study covered the period from December 01, 2020, until August 14,  
124 2021 (Figure 2).

### 125 **2.3.2 Weather data**

126 Precipitation and temperature data (Figure 3) with a 15 min temporal resolution were obtained from two weather stations  
127 located in the Eastern and Western end of the main patchCROP field. Climatic water balance was calculated from precipitation  
128 and potential evapotranspiration, both measured at the climate station by the German Weather Service in Müncheberg (DWD  
129 Climate Data Center (CDC), 2021). This station was chosen due to its proximity to the study site.

### 130 **2.3.3 Remote senses data for vegetation dynamics**

131 Furthermore, drone imagery from May 20, 2021, May 31, 2021, and July 06, 2021, was used for vegetation assessment. The  
132 drone fixed-wing UAV-based RS eBee platform (SenseFly Ltd., Cheseaux-Lausanne, Switzerland) was operated at noon time  
133 and recorded multispectral imagery with a Parrot Sequoia+ camera (green, red, NIR, and red edge bands, spatial resolution of  
134 0.105 m) and thermal imagery of the surface (only on May 31, 2021) with a senseFly Duet T camera with a spatial resolution  
135 of 0.091 m (Table 2). The multispectral imagery was processed with Pix4D to obtain the Normalized Difference Vegetation  
136 Index (NDVI), following Eq. (1):

$$137 \quad NDVI = \frac{NIR-Red}{NIR+Red} \quad (1)$$

138 in which NIR is the intensity of reflected near-infrared light (reflected by vegetation) and Red the intensity of reflected red  
139 light (absorbed by vegetation). A digital elevation model with a spatial resolution of 1 m (GeoBasis-DE and LGB, 2021) was  
140 used to calculate the slope (ArcGIS 10.7.0; ESRI, 2011) (Table 2).

### 141 **2.3.4 Soil information**

#### 142 *Soil texture by layer*

143 Manual classification of soil texture by layer was carried out by collecting 140 samples in eight of twelve analysed patches.  
144 Samples were taken with a 1 m-length Pürckhauer soil auger. Soil textural class was manually determined at the field by  
145 applying the protocol “Finger test to determine soil texture according to DIN 19682-2 and KA5” (Sponagel et al., 2005).  
146 Additionally, representative soil samples were collected and analysed at the laboratory to determine particle size distribution  
147 for sand, silt, and clay (soil texture based on the German particle classification). Soil texture was analysed following the DIN  
148 ISO 11277 (2002) reference method by wet sieving and sedimentation, using the SEDIMAT 4-12 (Umwelt-Geräte-Technik  
149 GmbH, Germany). The sand fraction in this method is defined between 2 and 0.063 mm, according to IUSS Working Group  
150 WRB (2015).

151 To extrapolate the laboratory-based soil particle distribution to the soil textural classes manually determined at the field the  
152 high and low yield potential laboratory samples were pooled separately. The average soil particle distribution was calculated  
153 for each soil textural class and assigned to the respective soil layer with that specific soil textural class. The soil texture analysis  
154 showed that soil texture variability increased with depth. In the third layer (average bottom depth = 0.92 m), the sand and clay

155 content across 133 sampling points varied between 53% to 94% and 2% to 22%, respectively. Soil sampling points were  
156 located 0.8 m and 2.5 m away from the soil moisture sensors to minimize damage risk.

### 157 *Topsoil proximally sensed data*

158 In October 2019, the “Geophilus” soil scanner system (Lueck and Ruehlmann, 2013) was used in the entire field to map soil  
159 electrical resistivity (ERa) as a proxy for texture for the top soil, using reference soil samples to calibrate the readings. A total  
160 of four georeferenced reference soil samples were taken until 0.25 m soil depth, and locations were selected based on the  
161 proximal soil sensor data (sensor-guided sampling; Bönecke et al., 2021). The “Geophilus” system is based on sensor fusion  
162 in which ERa sensors are coupled with a gamma-ray detector. Apparent electrical conductivity was measured by pulling one  
163 or more sensor pairs mounted on wheels across the field where each pair of sensors measured a different soil depth. Amplitude  
164 and phase were measured simultaneously using frequencies from 1 MHz to 1 kHz. Reference soil samples were analysed via  
165 soil-particle size analysis according to DIN ISO 11277 (2002) and served as calibration information in order to estimate sand,  
166 silt and clay content in the top 0.25 m soil for the entire field. A non-linear regression model was applied. The RMSE of sand  
167 content (5.7%) was considerably smaller than the standard deviation of the sand content in the first layer from the manual soil  
168 texture analysis (11.9%), indicating a satisfactory prediction performance. The gamma-sensor was used to minimize  
169 uncertainties, being less sensitive to soil moisture than the ERa readings (Bönecke et al., 2021). The estimated sand content in  
170 the upper 0.25 m at the study site varied between 69.1% and 81.2% and averaged 79.0% (Table 1, Figure 1).

### 171 **2.4 Data processing**

172 Soil moisture data were available at 20-minute intervals. Transmission failures due to discharged batteries, signal disturbances  
173 after rainfall, in patches with a high density of biomass (e.g. maize), and theft of parts of the WSN led to data gaps that affected  
174 in some cases all sensors of the WSN and amounted to 81 out of 257 days of the measuring period. The affected days were  
175 therefore skipped for the analysis. Whereas time series of eight sensors were excluded due to a higher frequency of transmission  
176 failures, in total, 64 time series were used for the analysis, and additional data gaps for single sensors were interpolated linearly.  
177 Of all 20,668 interpolated gaps, 96% were shorter than two hours, 3% between two and six hours and 1% longer than six hours.  
178 In 26 cases, gaps exceeded the duration of one day. The interpolation was justified as the differences between the values before  
179 and after the gaps were within the measuring accuracy of 1 vol-% of the soil moisture sensors (Acclima Inc., 2019). As  
180 indicated by the retailer, sensors might suddenly jump to a soil moisture value of 28.6% and go back to normal again after one  
181 or few time steps. Thus, a data deletion procedure of abrupt jumps to 28.6 was created. To ensure equal weighting for the  
182 subsequent analysis, all soil moisture time series were z-transformed to unit variance and zero mean each (cf. Hohenbrink and  
183 Lischeid, 2015). As a consequence, differences of absolute values were not considered by the further analysis.

## 184 **2.5 Statistical analysis**

185 To identify common temporal patterns among single time series, the soil moisture data set was analysed by a principal  
186 component analysis (PCA). In a first step, PCA decomposes the total variance of a multivariate data set into independent  
187 fractions called principal components (PCs). The number of PCs is the same as the number of time series in the input data set.  
188 Each PC consists of eigenvectors (loadings), scores, and eigenvalues. The scores reflect the temporal dynamics. The  
189 importance of single principal components for single sites is represented by the loadings of each PC (Jolliffe, 2002; Lehr and  
190 Lischeid, 2020). Loadings are the Pearson correlation coefficients of the single time series of the input data set with the scores  
191 of each PC, respectively. The eigenvalues of the single PC are proportional to the variance that they explain. The PCs are  
192 sorted in descending order of eigenvalues. Eigenvalues greater than one indicate that a PC explains more variance than a single  
193 input time series could contribute to the total variance of the entire input data set (Kaiser, 1960). More details on principal  
194 component analysis for time series analysis are found in Jolliffe (2002). The PCA was performed using the *prcomp* function in  
195 R version 4.1.0 (R Development Core Team, 2021).

196 The scores of the principal components constitute time series. Every observed soil moisture z-transformed time series can be  
197 presented at arbitrary precision as a combination of various principal components. When the data set consists of time series of  
198 the same observable measured at different locations, the first principal component describes the mean behaviour inherent in  
199 the data set. Subsequent principal components reflect typical modifications of that mean behaviour at single locations due to  
200 different effects. Thus, generating synthetic time series as linear combinations of the first PC and another additional PC helps  
201 to assign this additional PC to a specific effect. To that end, scores of that component have either been added to or subtracted  
202 from those of the first component using arbitrarily selected factors. The two resulting graphs show how the respective PC  
203 causes deviations from the mean behaviour of the data set.

204 The relations to soil and vegetation parameters were tested by computing the Pearson correlation coefficients between the  
205 scores and arithmetic mean values of all input time series as well as the Pearson correlation coefficients between loadings and  
206 sand content until 0.25 m depth, sensor depth, antecedent z-transformed soil moisture, slope, and drone imagery products  
207 (NDVI and surface temperature). Eventually, the Wilcoxon-Mann-Whitney test was applied to check whether loadings can be  
208 grouped by management parameters (crops, cover crops, weeding management). All statistical analyses were conducted with  
209 R version 4.1.0 (R Development Core Team, 2021).

## 210 **3 Results**

### 211 **3.1 Manual soil texture analysis**

212 The transferability of texture information from the sampling point to the soil moisture sensor location was not ensured due to  
213 high nugget effects. Furthermore, manual soil texture analysis data were not available for all analysed patches. Consequently,  
214 they were not included into further analysis.

## 215 **3.2 Principal component analysis**

216 The principal component analysis yielded five components with Eigenvalues exceeding one, which accounted for >97% of the  
217 total variance of the data set (Table 3).

### 218 **3.2.1 First principal component**

219 The first principal component explained 72.3% spatiotemporal variance of the data set. All loadings on the first PC were  
220 negative (Appendix A). The Pearson correlation coefficient of the scores of the first principal component with the mean values  
221 of all input time series was less than - 0.999 ( $p < 0.01$ ), the correlation between the scores and the cumulative climatic water  
222 balance ( $P - ET_p$ ) was -0.969 ( $p < 0.01$ ). Thus, the time series of the negative scores of this component represented the mean  
223 behaviour of soil moisture driven by external factors such as precipitation, temperature, and seasons in general which affected  
224 time series in the same way, although to different degrees (cf., Hohenbrink et al., 2016; Lischeid et al., 2021).

### 225 **3.2.2 Second principal component**

226 The second principal component explained 17.0% of the total variance. The loadings ranged from -0.801 to 0.760 with a  
227 median of -0.030 (Figure 4). The loadings showed a crop group specific pattern. All winter crops (barley, oats, rye) had positive  
228 loadings with only one exception in 0.9 m depth. The summer crops maize, soy, and sunflower exhibited negative loadings. In  
229 contrast, the summer crop lupine exhibited mostly positive loadings, similar to the winter crops, although of slightly smaller  
230 magnitude. According to the Wilcoxon-Mann test, the group of barley, oats, rye, and lupine differed significantly from the  
231 group of maize, soy, and sunflower.

232 As described in the Methods section, synthetic time series were generated as a linear combination of PC1 and PC2 (Figure 5).  
233 The graph resulting from applying a positive factor for PC2 represents a typical deviation from mean behaviour for sites that  
234 exhibit positive loadings, e.g., winter crops (blue line). The opposite holds for the summer crops which load negatively with  
235 PC2 (orange line). Both lines plot very close to each other in February and March. In contrast, the orange line shows lower  
236 values than the blue line in December and January, indicating lower soil moisture at the summer crop patches. The inverse  
237 holds for the subsequent summer period starting in early June, pointing to earlier and more rapid water uptake of the winter  
238 crops. In July and August, the approximately constant level of the blue curve indicates that only summer crops continue to  
239 consume water while winter crops are in their ripening phase and eventually harvested.

240 Lupine and sunflower were the summer crops which were sown first (March 30, 2021, and April 2, 2021, respectively). Maize  
241 was sown on April 16, 2021, and soy on May 15, 2021. The loadings of lupine, which were rather performing like winter crops  
242 than summer crops, indicated that lupine showed an early onset of intensive evapotranspiration, compared to other summer  
243 crops, especially sunflower which was sown at the same time.

244 For further investigation of the vegetation effect on PCs, drone imagery taken at the end of May, when sowing has been  
245 completed in all patches, and imagery taken at the beginning of July, when winter crops are in the ripening phase, was analysed.  
246 The second PC's loadings of the time series from different sensors were compared to the Normalized Difference Vegetation



247 Index (NDVI; available for three dates) and surface temperature (only available for May 31, 2021) of the respective sensor  
248 location as a proxy for actual evapotranspiration. At the end of May, the NDVI, as a proxy for photosynthesis potential, was  
249 positively correlated with the loadings (Table 4). Surface temperature exhibited a negative correlation. The spatial pattern of  
250 surface temperature is assumed to be inversely related to that of actual evapotranspiration. Thus, both proxies, NDVI and  
251 surface temperature, support the inference that in this study positive loadings on this principal component represent sites with  
252 above-average plant activity and root water uptake at the end of May. This holds for sensors from all depths but was the closest  
253 for 0.9 m depth (Pearson correlation of  $r = -0.916$  for surface temperature and of  $r = 0.946$  for NDVI on May 31). The results  
254 in July compared to those in May support the observation. At the time when the winter crops are already in the ripening phase  
255 and the summer crops reach high levels of evapotranspiration, the correlations are being reversed and negative loadings  
256 indicate above-average plant activity for summer crops. On July 06, highest Pearson correlations for NDVI are found for 0.6  
257 m depth ( $r = -0.917$ ).

### 258 **3.2.3 Third principal component**

259 The third PC explained 4.1% of the total data set's variance. Loadings ranged between -0.787 and 0.244 with a median of  
260 0.006. Extreme loadings ( $<-0.25$ ) were found only for sensors in 0.9 m depth in patches 66, 89, 95 and 102 (Figure 6). The  
261 location of these patches shows a certain spatial pattern, with the patches roughly following an east-west direction rather than  
262 being distributed randomly within the field. This may point to topography or soil structure causing deviations from mean soil  
263 moisture behaviour for patches located near this gradient. However, this pattern cannot be assigned to topography or structures  
264 apparent on the topsoil map (Figure 1). Loadings were closely related to the minima of the z-transformed soil moisture in the  
265 period from December to February ( $r = 0.70$ ,  $p < 0.001$ , Figure 7). What distinguishes the orange line (negative loading on  
266 PC3) from the blue line (positive loading on PC3) is the higher temporal variability and the delayed reaching of maxima in  
267 the first half of the study period (Figure 8).

### 268 **3.2.4 Fourth principal component**

269 The fourth PC explained 2.2% of the total data set's variance. The loadings were clustered by crop groups. All fallow patches  
270 showed consistent positive loadings while the patches which were covered by winter crops, showed mainly negative loadings  
271 except in patch 95 where the loadings of the two sensors in 0.3 m depth were slightly above zero (Figure 9). According to the  
272 Wilcoxon-Mann test treatment group B (fallow, followed by summer crops) differed significantly from group A (winter crops)  
273 and C (cover crops, followed by summer crops) whereas there was no significant difference between group A and C. In contrast  
274 to crop groups A and B, patches that were covered by the cover crop phacelia during the winter months, did not show one-  
275 directional loadings.

276 Figure 10 illustrates the effect of the fourth PC on time series. The blue line (positive loading) shows a hydrological behaviour  
277 which would be typical for more sandy soils while the orange line (negative loading) depicts behaviour that one would expect  
278 in more loamy soils due to its delayed responses to rainstorms and subsequent less steep recovery. The patterns in the loadings

279 thus show a differentiation between patches with winter crops and fallow patches in the winter months (Figure 9). However,  
280 it is not clear how winter crops on the one side and fallow on the other side could induce such a different soil water behaviour  
281 shown in Figure 10.

### 282 **3.2.5 Fifth principal component**

283 The fifth PC explained 1.7% of the data set's variance. The loadings showed a depth-related pattern. All time series from the  
284 0.3 m depth exhibited negative loadings with two minor exceptions. Whereas all time series from 0.9 m depth showed positive  
285 loadings throughout, and time series from 0.6 m depth plot in between. Loadings in 0.6 m depth and 0.9 m depth were mostly  
286 more similar to each other than to the loadings of 0.3 m depth (Figure 11). The Pearson correlation coefficient between loadings  
287 and depth was  $r = 0.710$  ( $p < 0.05$ ). Thus it can be concluded that the fifth PC reflected the effect of soil depth on soil moisture  
288 variance. This effect differed between crops, with the three most negative loadings found in maize patches while the three  
289 most positive loadings were found in lupine patches. The soil water dynamics show a damping effect with increasing depth  
290 (Figure 12) from little damping for sensors in the upper depth (orange line) to higher damping for sensors in greater depth  
291 (blue line).

292 Neither patterns in topography nor in weeding management modes were reflected in the loadings of PC1-PC5. Due to the lack  
293 of subsurface soil data, no additional findings could be derived from the Geophilus texture analysis.

## 294 **4 Discussion**

295 A PCA was conducted to identify the drivers of soil moisture variability in a diversified cropping field. Data consisted of  
296 observed time series from 64 soil moisture probes. Results showed that the first five principal components described about  
297 97% of the variance of the data set, and revealed various effects of weather, soil texture, soil depth, crops and management  
298 schemes (Table 3). The first principal component captured 72% of the total variance. Consequently, 72% of the observed  
299 dynamics could be described by a lumped model that would not consider any within-field heterogeneity. These results are in  
300 the range of similar studies. Martini et al. (2017) found that the first PC explained 58% of the variance of a data set that  
301 comprised both agricultural fields as well as grassland transects. Similarly, Lischeid et al. (2017) ascribed 70% of the variance  
302 of a forest soil moisture data set to a single component. In the study by Hohenbrink et al. (2016), 85% of the variance of soil  
303 moisture data in a set of arable field experiments with two different crop rotation schemes was attributed to the first principal  
304 component. The strong influence of weather conditions as it is shown in our study is confirmed by Choi et al. (2007) who  
305 showed that rainfall, next to topography, explained most of the surface soil moisture variability.

### 306 **4.1 Crop effects**

307 As Korres et al. (2015) stated that vegetation and management (e.g. planting and harvesting dates) are among the main causes  
308 for spatial variability of soil moisture in agricultural fields. In this study, around 17% of the total variance at the field scale

309 was attributed to the vegetation effect. When not considering the temporal component reflected by PC1 and thus only looking  
310 at the spatial variability, 61% of the remaining variance is caused by the vegetation effect reflected by PC2. Korres et al. (2010)  
311 also used PCA to identify the drivers of spatial variability of soil moisture within a cropped area but did not find such a  
312 pronounced vegetation effect. In their study, more than two thirds of the spatial variability was related to soil parameters and  
313 topography. In contrast, the strong influence of vegetation in our study may be due to the high level of crop diversification.  
314 Within single crop fields, vegetation effects are observable due to heterogeneous biomass or root development (Brown et al.,  
315 2021; Korres et al., 2010), but may be of a lower magnitude compared to fragmented field arrangements with different crops.  
316 The high impact of crop diversification on soil moisture variability is also visible when comparing our results to the results of  
317 a field under comparable conditions in the same region with only two crop rotations in which only 3.8% was explained by the  
318 different crop rotations (Hohenbrink et al., 2016). Joshi and Mohanty (2010) also assessed the effect of vegetation in their  
319 study in which they investigated spatial soil moisture variability at the field to regional scale in the Southern Great Plains  
320 regions in the US by means of PCA . With none of the first seven PC showing strong correlation with vegetation parameters,  
321 the effect of vegetation was limited in contrast to our study.

322 It needs to be considered that the proportion of the vegetation effect on soil moisture variability does not only vary spatially  
323 and over depth, but also over time. Under dry conditions, soil-plant interactions prevail while under moist conditions,  
324 percolation behaviour is predominant (Baroni et al., 2013). The scores are time series and reflect the effect size of a particular  
325 process represented by the respective PC. The more the scores of a certain PC deviate from zero during specific periods, the  
326 stronger the respective effect is. Consequently, the time series of PC2 scores indicates that the effect of vegetation on total  
327 variability varies by time. In accordance with literature, the absolute values of the scores of PC2, representing differences  
328 between the contrasting seasonality of crops, are highest in the dry months, May to August. This is mostly explained by the  
329 high water demand of summer crops, which are in their vegetative growth stage from May to August, whereas winter crops  
330 are already in their reproductive growth stage, including maturity, senescence and harvest where water uptake by crops is  
331 minimal or absent (Zhao et al, 2018). In the moist winter months January to March, as well as during the heavy rainfall event  
332 in July, the scores of PC2 are relatively small, showing that spatial variability at that time is caused by other factors.

333 The second principal component clearly differentiated between winter and summer crops, which was driven by the different  
334 seasonal patterns of root water uptake (Figure 4). In contrast, the fourth component differentiated between fallow followed by  
335 summer crops and winter crops, whereas phacelia followed by summer crop did not show a clear pattern (Figure 9). Phacelia  
336 is grown as a cover crop and usually dies off in frost periods. Due to rather mild winter temperatures 2020/21, Phacelia was  
337 not terminated efficiently and kept growing until spring, until it was terminated mechanically. It was recently shown that the  
338 timing of removal of winter cover crops is key to provide soil water recharge for the subsequent crop, as the depletion of soil  
339 water in autumn is significant (Selzer and Schubert, 2023). Thus, some Phacelia patches exhibited negative loadings, similarly  
340 to the winter crop patches while other patches with most likely different termination dates exhibited positive loadings.

341 Hence, the fourth component obviously reflected the effect of the active root system in the winter period. According to this  
342 component, soil water dynamics in the fallow patches mostly resembled the typical behaviour expected for sandy soils, and

343 winter crop patches showed a more damped behaviour that is usually observed in more loamy soils. Note that the term “fallow”  
344 refers to crop cover in autumn and winter only. Acharya et al. (2019) found that winter cover crops increased soil moisture  
345 from 3% to 5% in the top 0.3 m soil layer which is in line with the findings from Figure 10 that shows a higher water holding  
346 capacity for winter crops (orange line) in winter. However, it has also been observed that roots from winter crops can increase  
347 soil porosity and therefore, water mobility in the soil (Lange et al., 2013; Scholl et al., 2014).  
348 Further soil-vegetation interactions might play a role for the delayed seepage fluxes of winter crop and part of cover crop  
349 patches, such as soil organic content increase through the presence of cover crops and plant residues (Manns et al., 2014;  
350 Rossini et al., 2021). Usually, such effects are assumed to occur only at larger time scales, which is closely related to problems  
351 of detecting changes soil organic carbon (SOC) quantity or quality. So far, there is only anecdotal evidence for rather short-  
352 term SOC quality affecting soil hydraulic properties even at smaller time scales. Although this effect constituted only a minor  
353 share of soil moisture variance (Table 3), it was clearly discernible as a separate principal component. This effect would be  
354 worth to be tested in more detailed future studies.

#### 355 **4.2 Soil texture and soil depth effects**

356 Loadings on the third principal component were not related to crop types. In contrast, a spatial pattern emerged: Only sensors  
357 from 0.9 m depth from six adjacent patches exhibited strongly negative loadings (Figure 6), whereas all other sensors showed  
358 minor positive or negative loadings. This points to an effect of subsoil substrates, that is, higher clay content and consequently  
359 higher water holding capacity. That would be consistent with delayed response to seepage fluxes and reduced desiccation in  
360 the vegetation period (Figure 8). The strong relation between z-transformed soil moisture minima at the beginning of the study  
361 period (Figure 7) which might originate from a delayed response to a prior rainfall, and the regional pattern of the location of  
362 the patches following a west-east direction within the experiment might be an indicator of underlying soil structures causing  
363 this effect. Data on texture at soil moisture sensor locations in deeper layers would be of high value to confirm the assumptions.  
364 Whereas the third principal component seems to reflect a local peculiarity, the fifth component obviously grasps a more generic  
365 feature. Loadings on this component are clearly related with depth (Figure 11). Strong positive loadings indicate a strongly  
366 damped behaviour of soil moisture time series: The blue line, representing sites with positive loadings on PC5 which is typical  
367 for sensors at greater depth (Figure 12), exhibits clearly reduced amplitudes compared to the orange line, that is, sensors at  
368 shallow depth. Hohenbrink and Lischeid (2015) combined a hydrological model and principal component analysis to study the  
369 effect of soil depth and soil texture on damping of the input signal in more detail. A subsequent field study proved the relevance  
370 of that effect in a real-world setting (Hohenbrink et al., 2016). Moreover, Thomas et al. (2012) found that damping accounted  
371 for a large share of variance in a set of hydrographs from a region of 30,000 km<sup>2</sup>. Damping was also the most relevant driver  
372 of spatial variance in a set of time series of groundwater head at about the same scale (Lischeid et al., 2021).

#### 373 **4.3 Limitations**

374 Data gaps during the studied period occurred due to multiple technical and environmental factors. Data gaps in soil moisture  
375 time series were caused by repeated temporary failure of the WSN. There was a failure of one sensor that was replaced and  
376 one LoRa node was damaged by intruding water. More relevant, however, were failures of data transmission. Yildiz et al.  
377 (2015) point to the problem of optimizing transmission power for data and acknowledgement packets depending on energy  
378 dissipation under the given conditions. E.g., saturated soil conditions and dense biomass stands reduce the transmission signal  
379 from the node to the gateway (Bogena et al., 2009). The installation of a second gateway in September 2021 increased higher  
380 transmission coverage in the field. Another obstacle was snow cover on the gateways' solar panels. Finally, solar panels were  
381 subject to theft. However, higher level of maintenance and supervision helped to reduce the number and the length of data  
382 gaps.

383 PCA requires gapless time series. Gaps in single time series need to be either filled at the risk of introducing artefacts or the  
384 respective time period cannot be considered at all for analysis. This can be seen as a weakness of PCA. On the other hand, and  
385 in contrast to other time series analysis approaches, the time series need not to be equidistant. Assigning PCs to processes and  
386 effects is not straightforward and might be subject for debate. For example, in this study soil samples were taken at least at 0.8  
387 m distance from the sensors to avoid disturbance of the measurements. Due to pronounced small-scale soil variability these  
388 samples are not fully representative for the measurement sites. In spite of these limitations, the PCA results clearly point to  
389 various effects worth to be studied in more detail in subsequent studies.

## 390 **5 Conclusion**

391 The use of PCA has a high value for the application in environmental sciences, as it contributes to process understanding of  
392 soil water dynamics by disentangling the different effects of complex spatially and temporally diversified cropping systems.  
393 In this study, more than 97% of the observed spatial and temporal variance was assigned to five different effects.  
394 Meteorological drivers explained 72.3% of the total variance (PC1). Different seasonal patterns of root water uptake of winter  
395 crops compared to summer crops accounted for another 17.0% of variance (PC2). An additional share of 2.2% of variance  
396 seemed to be related to the effects of different vegetation cover and its interplay with soil hydraulic properties (PC4).  
397 Heterogeneity of subsoil substrates explained 4.1 % of variance (PC3), and the damping effect of input signals over depth  
398 another 1.7% (PC5). To summarize, plant-related direct and indirect effects accounted for 19.2% of the variance (PC2 and  
399 PC4), and soil-related effects only for 5.8% (PC3 and PC5). In particular, the plant-induced effects on soil hydraulic properties  
400 would be worthwhile to be studied in more detail.

401 Findings of this study highly depend on local conditions. However, the methodology itself is generally applicable to other site  
402 conditions and can lead to improved management practices through improved knowledge about soil water dynamics.  
403 Furthermore, information from this study can also help to develop both parsimonious and tailored mechanistic models for  
404 model upscaling. In this regard, principal component analysis of large soil moisture data sets from real-world monitoring setups  
405 performed a meaningful diagnostic tool for complex cropping systems.

406 **Data availability**

407 The analysed soil moisture dataset is available under <https://doi.org/10.4228/zalf-3rsc-6c30>.

408 **Author contribution**

409 KG designed the study, implemented the sensor network and data monitoring program, supervised the project and acquired  
410 the additional financial support for the project leading to this publication; GL, KG and HS conceptualized the analysis; HS  
411 processed the experimental data, analysed the data and designed the figures; IHO performed the manually collected soil data  
412 campaign; HS wrote the manuscript draft with contributions from all co-authors; GL, KG, IHO, HS and LR reviewed and  
413 edited the manuscript.

414 **Competing interests**

415 The authors declare that they have no conflict of interest.

416 **Acknowledgments**

417 The maintenance of the patchCROP experimental infrastructure and the LoRaWAN soil sensor system is ensured by the  
418 Leibniz Centre for Agricultural Landscape Research. The authors acknowledge the additional support from the German  
419 Research Foundation under Germany's Excellence Strategy, EXC-2070 – 390732324 – PhenoRob for patchCROP related  
420 research activities.

421 The authors would like to thank Gerhard Kast, Thomas von Oepen, Lars Richter, Robert Zieciak, Sigrid Ehlert and Motaz  
422 Abdelaziz for their dedicated support in maintenance of the monitoring system and data collection.

423 The authors would also like to thank the reviewers for their valuable contribution to this manuscript.

424 **References**

425 Acclima Inc.: True TDR310H. Soil-Water-Temperature-BEC-Sensor, 2019.

426 Acharya, B. S., Dodla, S., Gaston, L. A., Darapuneni, M., Wang, J. J., Sepat, S., and Bohara, H.: Winter cover crops effect on  
427 soil moisture and soybean growth and yield under different tillage systems, *Soil and Tillage Research*, 195,  
428 <https://doi.org/10.1016/j.still.2019.104430>, 2019.

429 Alhameid, A., Singh, J., Sekaran, U., Ozlu, E., Kumar, S., and Singh, S.: Crop rotational diversity impacts soil physical and  
430 hydrological properties under long-term no- and conventional-till soils, *Soil Res.*, 58, 84, <https://doi.org/10.1071/SR18192>,  
431 2020.

- 432 Baroni, G., Ortuani, B., Facchi, A., and Gandolfi, C.: The role of vegetation and soil properties on the spatio-temporal  
433 variability of the surface soil moisture in a maize-cropped field, *Journal of Hydrology*, 489, 148–159,  
434 <https://doi.org/10.1016/j.jhydrol.2013.03.007>, 2013.
- 435 BIRTHAL, P. S. and Hazrana, J.: Crop diversification and resilience of agriculture to climatic shocks: Evidence from India,  
436 *Agricultural Systems*, 173, 345–354, <https://doi.org/10.1016/j.agsy.2019.03.005>, 2019.
- 437 Bogena, H. R., Huisman, J. A., Meier, H., and Weuthen, A.: Hybrid wireless underground sensor networks: Quantification of  
438 signal attenuation in soil, *Vadose Zone J.*, 8, 755–761, <https://doi.org/10.2136/vzj2008.0138>, 2009.
- 439 Bogena, H. R., Weuthen, A., and Huisman, J. H.: Recent Developments in Wireless Soil Moisture Sensing to Support Scientific  
440 Research and Agricultural Management, *Sensors*, 22, 9792, <https://doi.org/10.3390/s22249792>, 2022.
- 441 Bönecke, E., Meyer, S., Vogel, S., Schröter, I., Gebbers, R., Kling, C., Kramer, E., Lück, K., Nagel, A., Philipp, G., Gerlach,  
442 F., Palme, S., Scheibe, D., Zieger, K., Rühlmann, J.: Guidelines for precise lime management based on high-resolution soil  
443 pH, texture and SOM maps generated from proximal soil sensing data, *Precision Agric*, 22, 493–523,  
444 <https://doi.org/10.1007/s11119-020-09766-8>, 2021.
- 445 Bretherton, C. S., Smith, C., and Wallace, J. M.: An intercomparison of methods for finding coupled patterns in climate data,  
446 *Journal of Climatology*, 5, 541–560, 1992.
- 447 Brocca, L., Melone, F., Moramarco, T., and Morbidelli, R.: Spatial-temporal variability of soil moisture and its estimation  
448 across scales, *Water Resour. Res.*, 46, <https://doi.org/10.1029/2009WR008016>, 2010.
- 449 Brown, M., Heinse, R., Johnson-Maynard, J., and Huggins, D.: Time-lapse mapping of crop and tillage interactions with soil  
450 water using electromagnetic induction, *Vadose zone j.*, 20, <https://doi.org/10.1002/vzj2.20097>, 2021.
- 451 Cardell-Oliver, R., Hübner, C., Leopold, M., and Beringer, J.: Dataset: LoRa Underground Farm Sensor Network, in:  
452 Proceedings of the 2nd Workshop on Data Acquisition To Analysis - DATA'19, the 2nd Workshop, New York, NY, USA,  
453 26–28, <https://doi.org/10.1145/3359427.3361912>, 2019.
- 454 Choi, M., Jacobs, J. M., and Cosh, M. H.: Scaled spatial variability of soil moisture fields, *Geophys. Res. Lett.*, 34,  
455 <https://dx.doi.org/10.1029/2006GL028247>, 2007.
- 456 Deumlich, D., Ellerbrock, R. H., and Frielinghaus, Mo.: Estimating carbon stocks in young moraine soils affected by erosion,  
457 *CATENA*, 162, 51–60, <https://doi.org/10.1016/j.catena.2017.11.016>, 2018.
- 458 Donat, M., Geistert, J., Grahmann, K., Bloch, R., and Bellingrath-Kimura, S. D.: Patch cropping- a new methodological  
459 approach to determine new field arrangements that increase the multifunctionality of agricultural landscapes, *Computers and*  
460 *Electronics in Agriculture*, 197, 106894, <https://doi.org/10.1016/j.compag.2022.106894>, 2022.
- 461 DIN ISO 11277: Soil quality - Determination of particle size distribution in mineral soil material - Method by sieving and  
462 sedimentation (ISO 11277:1998 + ISO 11277:1998 Corrigendum 1:2002), Beuth-Verlag, Berlin,  
463 <https://dx.doi.org/10.31030/9283499>, 2002.
- 464 DWD Climate Data Center (CDC): Historische tägliche Stationsbeobachtungen (Temperatur, Druck, Niederschlag,  
465 Sonnenscheindauer, etc.) für Deutschland, Version v21.3, 2021.
- 466 Fischer, C., Roscher, C., Jensen, B., Eisenhauer, N., Baade, J., Attinger, S., Scheu, S., Weisser, W. W., Schumacher, J.,  
467 Hildebrandt, A.: How Do Earthworms, Soil Texture and Plant Composition Affect Infiltration along an Experimental Plant  
468 Diversity Gradient in Grassland?, *PLoS ONE*, 9, 6, <https://doi.org/10.1371/journal.pone.0098987>, 2014.

- 469 Fischer, G. F., Nachtergaele, S., Prieler, S., van Velthuisen, H. T., Verelst, L., and Wisberg, D.: Global Agro-ecological Zones  
470 Assessment for Agriculture (GAEZ 2008), IIASA, Laxenburg, Austria and FAO, Rome, 2008.
- 471 GeoBasis-DE and Landesvermessung und Geobasisinformation Brandenburg (LGB): Digitales Geländemodell (DGM),  
472 Landesvermessung und Geobasisinformation Brandenburg (LGB), Potsdam, 2021.
- 473 Graf, A., Bogena, H. R., Drüe, C., Herdelauf, H., Pütz, T., Heinemann, G., and Vereecken, H.: Spatiotemporal relations  
474 between water budget components and soil water content in a forested tributary catchment, *Water Resour. Res.*, 50, 4837-  
475 4857, <https://doi.org/10.1002/2013WR014516>, 2014.
- 476 Grahmann, K., Reckling, M., Hernandez-Ochoa, I., Bellingrath-Kimura, S., and Ewert, F.: Co-designing a landscape  
477 experiment to investigate diversified cropping systems, *Agricultural Systems*, 217, 103950,  
478 <https://doi.org/10.1016/j.agsy.2024.103950>, 2024.
- 479 Hohenbrink, T. L. and Lischeid, G.: Does textural heterogeneity matter? Quantifying transformation of hydrological signals  
480 in soils, *Journal of Hydrology*, 523, 725–738, <https://doi.org/10.1016/j.jhydrol.2015.02.009>, 2015.
- 481 Hohenbrink, T. L., Lischeid, G., Schindler, U., and Hufnagel, J.: Disentangling the Effects of Land Management and Soil  
482 Heterogeneity on Soil Moisture Dynamics, *Vadose Zone Journal*, 15, <https://doi.org/10.2136/vzj2015.07.0107>, 2016.
- 483 Hupet, F. and Vanclooster, M.: Intraseasonal dynamics of soil moisture variability within a small agricultural maize cropped  
484 field, *Journal of Hydrology*, 261, 86–101, 2002.
- 485 IUSS Working Group WRB: World Reference Base for Soil Resources 2014, Update 2015, International Soil Classification  
486 System for Naming Soils and Creating Legends for Soil Maps, World Soil Resources Reports No. 106, Rome: FAO, 2015.
- 487 Jolliffe, I. T.: Principal component analysis. Springer Series in Statistics, Springer, New York, 2002.
- 488 Joshi, C. and Mohanty, B. P.: Physical controls of near-surface soil moisture across varying spatial scales in an agricultural  
489 landscape during SMEX02: Physical controls of soil moisture, *Water Resour. Res.*, 46,  
490 <https://doi.org/10.1029/2010WR009152>, 2010.
- 491 Kaiser, H. F.: The Application of Electronic Computers to Factor Analysis, *Educ. Psychol. Measur.*, 20,  
492 <https://doi.org/10.1177/001316446002000116>, 1960.
- 493 Karlen, D. L., Hurley, E. G., Andrews, S. S., Cambardella, C. A., Meek, D. W., Duffy, M. D., and Mallarino, A. P.: Crop  
494 Rotation Effects on Soil Quality at Three Northern Corn/Soybean Belt Locations, *Agron.j.*, 98, 484–495,  
495 <https://doi.org/10.2134/agronj2005.0098>, 2006.
- 496 Khan, H., Farooque, A. A., Acharya, B., Abbas, F., Esau, T. J., and Zaman, Q. U.: Delineation of Management Zones for Site-  
497 Specific Information about Soil Fertility Characteristics through Proximal Sensing of Potato Fields, *Agronomy*, 10, 1854,  
498 <https://doi.org/10.3390/agronomy10121854>, 2020.
- 499 Korres, W., Koyama, C. N., Fiener, P., and Schneider, K.: Analysis of surface soil moisture patterns in agricultural landscapes  
500 using Empirical Orthogonal Functions, *Hydrol. Earth Syst. Sci.*, 14, 751–764, <https://doi.org/10.5194/hess-14-751-2010>, 2010.
- 501 Korres, W., Reichenau, T. G., Fiener, P., Koyama, C. N., Bogena, H. R., Cornelissen, T., Baatz, R., Herbst, M., Diekkrüger,  
502 B., Vereecken, H., and Schneider, K.: Spatio-temporal soil moisture patterns – A meta-analysis using plot to catchment scale  
503 data, *Journal of Hydrology*, 520, 326–341, <https://doi.org/10.1016/j.jhydrol.2014.11.042>, 2015.
- 504 Koudahe, K., Allen, S. C., Djaman, K.: Critical review of the impact of cover crops on soil properties, *International Soil and*  
505 *Water Conservation Research*, 10, 343-354, <https://doi.org/10.1016/j.iswcr.2022.03.003>, 2022.

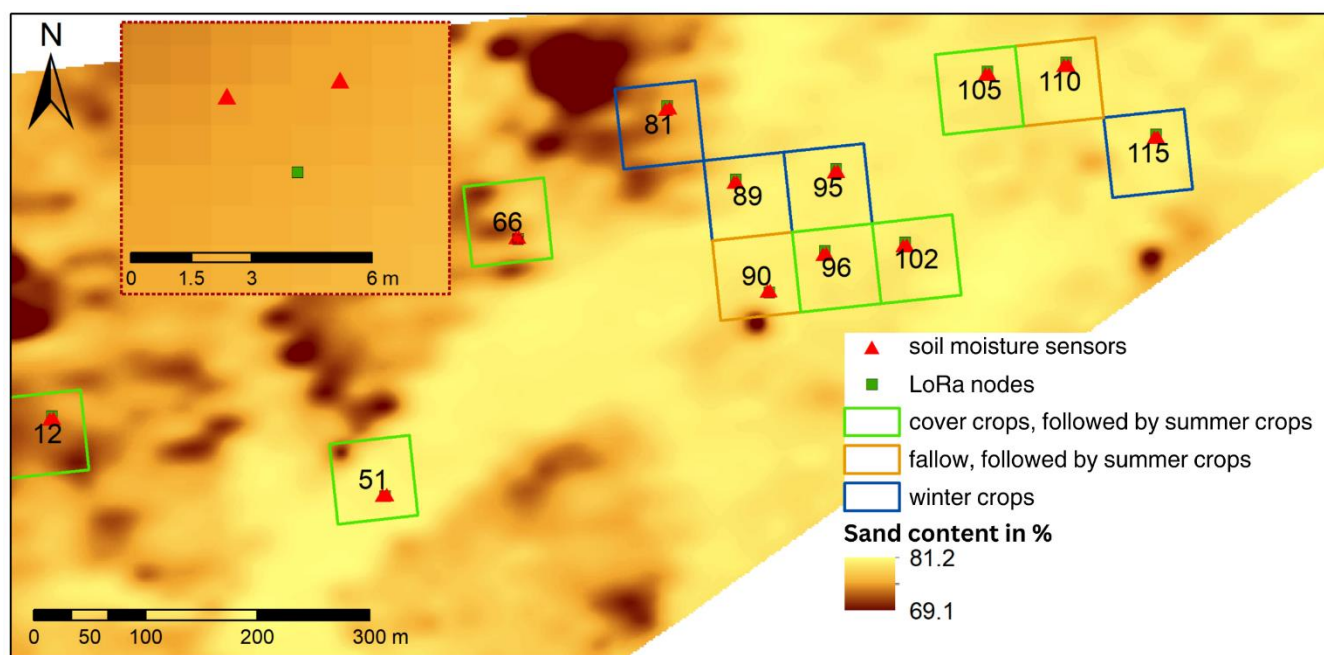


- 506 Krauss, L., Hauck, C., and Kottmeier, C.: Spatio-temporal soil moisture variability in Southwest Germany observed with a  
507 new monitoring network within the COPS domain, *metz*, 19, 523–537, <https://doi.org/10.1127/0941-2948/2010/0486>, 2010.
- 508 Lange, B., Germann, P. F., and Lüscher, P.: Greater abundance of *Fagus sylvatica* in coniferous flood protection forests due  
509 to climate change: impact of modified root densities on infiltration, *Eur J Forest Res*, 132, 151–163,  
510 <https://doi.org/10.1007/s10342-012-0664-z>, 2013.
- 511 Lehr, C. and Lischeid, G.: Efficient screening of groundwater head monitoring data for anthropogenic effects and measurement  
512 errors, *Hydrol. Earth Syst. Sci.*, 24, 501–513, <https://doi.org/10.5194/hess-24-501-2020>, 2020.
- 513 Lischeid, G., Frei, S., Huwe, B., Bogner, C., Lüers, J., Babel, W., and Foken, T.: Catchment Evapotranspiration and Runoff,  
514 in: *Energy and Matter Fluxes of a Spruce Forest Ecosystem*, vol. 229, Springer, Cham, Cham, 355–375, 2017.
- 515 Lischeid, G., Dannowski, R., Kaiser, K., Nützmann, G., Steidl, J., and Stüve, P.: Inconsistent hydrological trends do not  
516 necessarily imply spatially heterogeneous drivers, *Journal of Hydrology*, 596, 126096,  
517 <https://doi.org/10.1016/j.jhydrol.2021.126096>, 2021.
- 518 Lloret, J., Sendra, S., Garcia, L., and Jimenez, J. M.: A Wireless Sensor Network Deployment for Soil Moisture Monitoring  
519 in Precision Agriculture, *Sensors*, 21, 7243, <https://doi.org/10.3390/s21217243>, 2021.
- 520 Lueck, E. and Ruehlmann, J.: Resistivity mapping with *Geophilus Electricus* - Information about lateral and vertical soil  
521 heterogeneity, *Geoderma*, 199, 2–11, <https://doi.org/10.1016/j.geoderma.2012.11.009>, 2013.
- 522 Mahmood, R., Littell, A., Hubbard, K. G., and You, J.: Observed data-based assessment of relationships among soil moisture  
523 at various depths, precipitation, and temperature, *Applied Geography*, 34, 255–264,  
524 <https://doi.org/10.1016/j.apgeog.2011.11.009>, 2012.
- 525 Martini, E., Wollschläger, U., Musolff, A., Werban, U., and Zacharias, S.: Principal Component Analysis of the Spatiotemporal  
526 Pattern of Soil Moisture and Apparent Electrical Conductivity, *Vadose Zone J*, 16, vzj2016.12.0129,  
527 <https://doi.org/10.2136/vzj2016.12.0129>, 2017.
- 528 Nied, M., Hundecha, Y., and Merz, B.: Flood-initiating catchment conditions: a spatio-temporal analysis of large-scale soil  
529 moisture patterns in the Elbe River basin, *Hydrol. Earth Syst. Sci.*, 17, 1401–1414, <https://doi.org/10.5194/hess-17-1401-2013>,  
530 2013.
- 531 Nunes, M. R., van Es, H. M., Schindelbeck, R., Ristow, A. J., Ryan, M.: No-till and cropping system diversification improve  
532 soil health and crop yield, *Geoderma*, 328, 30–43, <https://doi.org/10.1016/j.geoderma.2018.04.031>, 2018.
- 533 Pan, F. and Peters-Lidard, C. D.: On the Relationship Between Mean and Variance of Soil Moisture Fields, *JAWRA Journal*  
534 *of the American Water Resources Association*, 44, 235–242, <https://doi.org/10.1111/j.1752-1688.2007.00150.x>, 2008.
- 535 Paroda, Raj. S., Suleimenov, M., Yusupov, H., Kireyev, A., Medeubayev, R., Martynova, L., and Yusupov, K.: Crop  
536 Diversification for Dryland Agriculture in Central Asia, in: *CSSA Special Publications*, edited by: Rao, S. C. and Ryan, J.,  
537 *Crop Science Society of America and American Society of Agronomy*, Madison, WI, USA, 139–150,  
538 <https://doi.org/10.2135/cssaspecpub32.c9>, 2015.
- 539 Placidi, P., Morbidelli, R., Fortunati, D., Papini, N., Gobbi, F., and Scorzoni, A.: Monitoring Soil and Ambient Parameters in  
540 the IoT Precision Agriculture Scenario: An Original Modeling Approach Dedicated to Low-Cost Soil Water Content Sensors,  
541 *Sensors*, 21, 5110, <https://doi.org/10.3390/s21155110>, 2021.
- 542 Prakosa, S. W., Faisal, M., Adhitya, Y., Leu, J.-S., Köppen, M., and Avian, C.: Design and Implementation of LoRa Based  
543 IoT Scheme for Indonesian Rural Area, *Electronics*, 10, 77, <https://doi.org/10.3390/electronics10010077>, 2021.

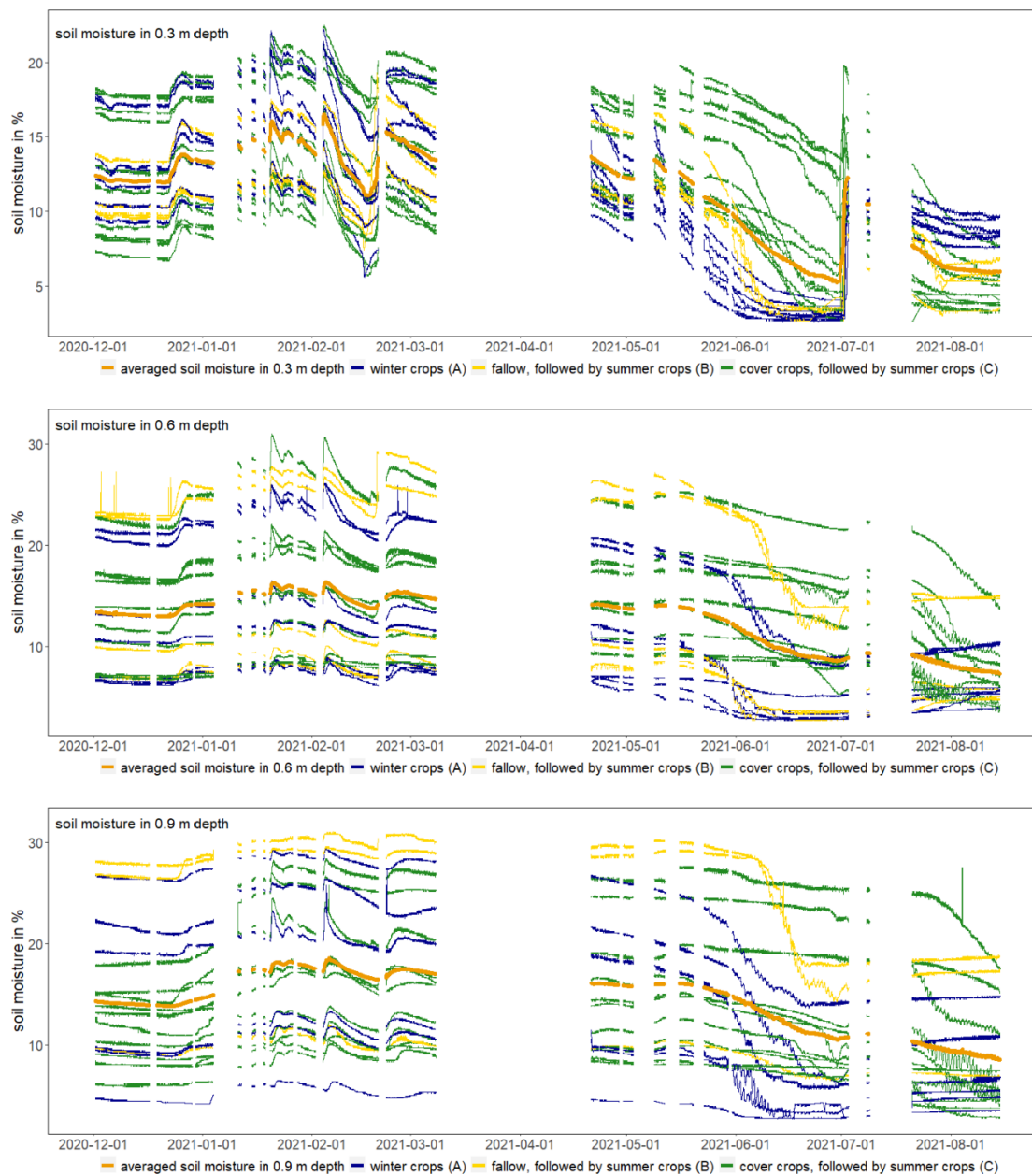
- 544 R Development Core Team: R: A Language and Environment for Statistical Computing, R Foundation for Statistical  
545 Computing (Version 4.1.0, <http://www.R-project.org>), Vienna, 2021.
- 546 Rodriguez, C., Mårtensson, L.-M. D., Jensen, E. S., and Carlsson, G.: Combining crop diversification practices can benefit  
547 cereal production in temperate climates, *Agron. Sustain. Dev.*, 41, 48, <https://doi.org/10.1007/s13593-021-00703-1>, 2021.
- 548 Rossini, P. R., Ciampitti, I. A., Hefley, T., and Patrignani, A.: A soil moisture-based framework for guiding the number and  
549 location of soil moisture sensors in agricultural fields, *Vadose zone J.*, 20, <https://doi.org/10.1002/vzj2.20159>, 2021.
- 550 Salam, A.: *Internet of Things for Sustainable Community Development: Wireless Communications, Sensing, and Systems*,  
551 Springer International Publishing, Cham, Switzerland, <https://doi.org/10.1007/978-3-030-35291-2>, 2020.
- 552 Salam, A. and Raza, U.: *Signals in the Soil: Developments in Internet of Underground Things*, Springer International  
553 Publishing, Cham, Switzerland, <https://doi.org/10.1007/978-3-030-50861-6>, 2020.
- 554 Scheffer, F. and Schachtschabel, P.: *Lehrbuch der Bodenkunde*, 15th ed., Spektrum Akademischer Verlag GmbH. Berlin,  
555 Heidelberg, <https://doi.org/10.1007/978-3-662-55871-3>, 2002.
- 556 Scholl, P., Leitner, D., Kammerer, G., Loiskandl, W., Kaul, H.-P., and Bodner, G.: Root induced changes of effective 1D  
557 hydraulic properties in a soil column, *Plant Soil*, 381, 193–213, <https://doi.org/10.1007/s11104-014-2121-x>, 2014.
- 558 Selzer, T., and Schubert, S.: Water dynamics of cover crops: No evidence for relevant water input through occult precipitation,  
559 *J Agro Crop Sci.*, 209, 422-437, <https://doi.org/10.1111/jac.12631>, 2023.
- 560 Si, B. C.: *Spatial Scaling Analyses of Soil Physical Properties: A Review of Spectral and Wavelet Methods*, *Vadose Zone*  
561 *Journal*, 7, 547–562, <https://doi.org/10.2136/vzj2007.0040>, 2008.
- 562 Sponagel, H., Grotenthaler, W., Hartmann, K.J., Hartwich, R., Janetzko, P., Joisten, H., Kühn, D., Sabel, K.J., Traidl, R.  
563 (Eds.): *Bodenkundliche Kartieranleitung (German Manual of Soil Mapping, KA5)*, 5<sup>th</sup> edition, Bundesanstalt für  
564 Geowissenschaften und Rohstoffe, Hannover, 2005.
- 565 Strebelle, S., Payrazyan, K., and Caers, J.: Modeling of a Deepwater Turbidite Reservoir Conditional to Seismic Data Using  
566 Principal Component Analysis and Multiple-Point Geostatistics, *SPE Journal*, 8, 227–235, <https://doi.org/10.2118/85962-PA>,  
567 2003.
- 568 Tamburini, G., Bommarco, R., Wanger, T. C., Kremen, C., van der Heijden, M. G. A., Liebman, M., and Hallin, S.:  
569 Agricultural diversification promotes multiple ecosystem services without compromising yield, *Sci. Adv.*, 6, eaba1715,  
570 <https://doi.org/10.1126/sciadv.aba1715>, 2020.
- 571 Taylor, J. and Whelan, B.: *A General Introduction to Precision Agriculture*, 2010.
- 572 Thomas, B., Lischeid, G., Steidl, J., and Dannowski, R.: Regional catchment classification with respect to low flow risk in a  
573 Pleistocene landscape, *Journal of Hydrology*, 475, 392–402, <https://doi.org/10.1016/j.jhydrol.2012.10.020>, 2012.
- 574 Trnka, M., Rötter, R. P., Ruiz-Ramos, M., Kersebaum, K. C., Olesen, J. E., Žalud, Z., and Semenov, M. A.: Adverse weather  
575 conditions for European wheat production will become more frequent with climate change, *Nature Clim Change*, 4, 637–643,  
576 <https://doi.org/10.1038/nclimate2242>, 2014.
- 577 Vachaud, G., Passerat De Silans, A., Balabanis, P., Vauclin, M.: Temporal Stability of Spatially Measured Soil Water  
578 Probability Density Function, *Soil Science Society of America Journal*, 49, 822-828,  
579 <https://doi.org/10.2136/sssaj1985.03615995004900040006x>, 1985.

- 580 Vanderlinden, K., Vereecken, H., Hardelauf, H., Herbst, M., Martínez, G., Cosh, M. H., Pachepsky, Y. A.: Temporal Stability  
 581 of Soil Water Contents: A Review of Data and Analyses, *Vadose Zone J.*, <https://doi.org/10.2136/vzj2011.0178>, 2012.
- 582 Vereecken, H., Huisman, J. A., Pachepsky, Y., Montzka, C., van der Kruk, J., Bogena, H., Weihermüller, L., Herbst, M.,  
 583 Martínez, G., and Vanderborght, J.: On the spatio-temporal dynamics of soil moisture at the field scale, *Journal of Hydrology*,  
 584 516, 76–96, <https://doi.org/10.1016/j.jhydrol.2013.11.061>, 2014.
- 585 Yang, L., Chen, L., and Wei, W.: Effects of vegetation restoration on the spatial distribution of soil moisture at the hillslope  
 586 scale in semi-arid regions, *CATENA*, 124, 138–146, <https://doi.org/10.1016/j.catena.2014.09.014>, 2015.
- 587 Yildiz, H. U., Tavli, B., and Yanikomeroglu, H.: Transmission power control for link-level handshaking in wireless sensor  
 588 networks, *IEEE Sensors Journal*, 16, 2, 561-576. 2015.
- 589 Zhao, X., Li, F., Ai, Z., Li, J., and Gu, C.: Stable isotope evidences for identifying crop water uptake in a typical winter wheat–  
 590 summer maize rotation field in the North China Plain, *Science of The Total Environment*, 618, 121-131,  
 591 <https://doi.org/10.1016/j.scitotenv.2017.10.315>, 2018.
- 592 Zhao, Y., Peth, S., Wang, X. Y., Lin, H., and Horn, R.: Controls of surface soil moisture spatial patterns and their temporal  
 593 stability in a semi-arid steppe, *Hydrol. Process.*, 24, 2507–2519, <https://doi.org/10.1002/hyp.7665>, 2010.

594 **Figures and Tables**

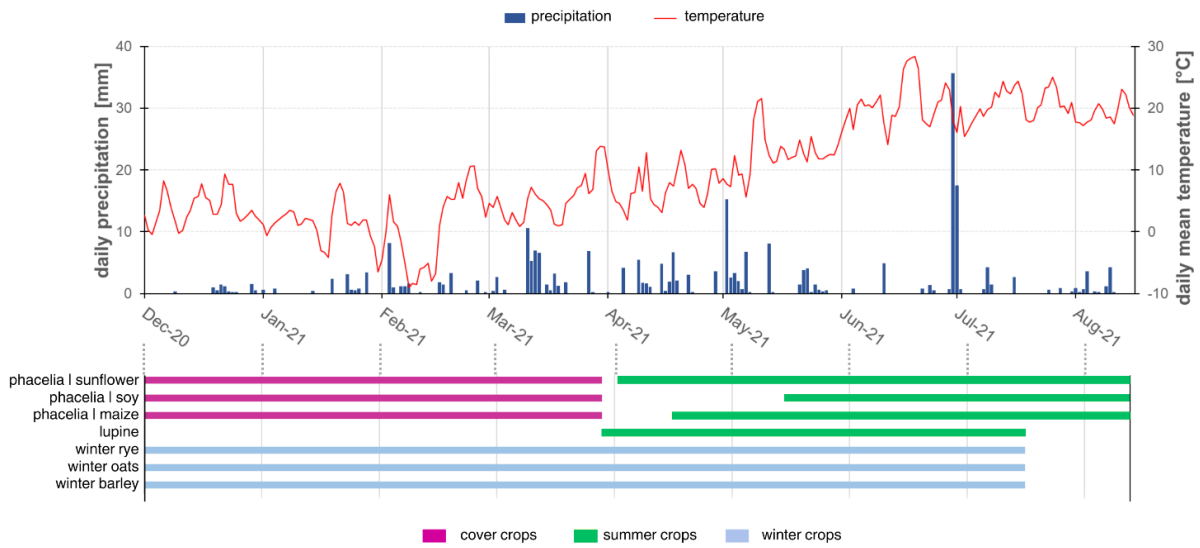


596 **Figure 1: Sand content in % in the top 0.25 m soil depth, location of the analysed patches, soil sensors (triangle) and boxes**  
 597 **(square) under different crop rotations at the patchCROP landscape laboratory, Tempelberg, Brandenburg, Germany.**



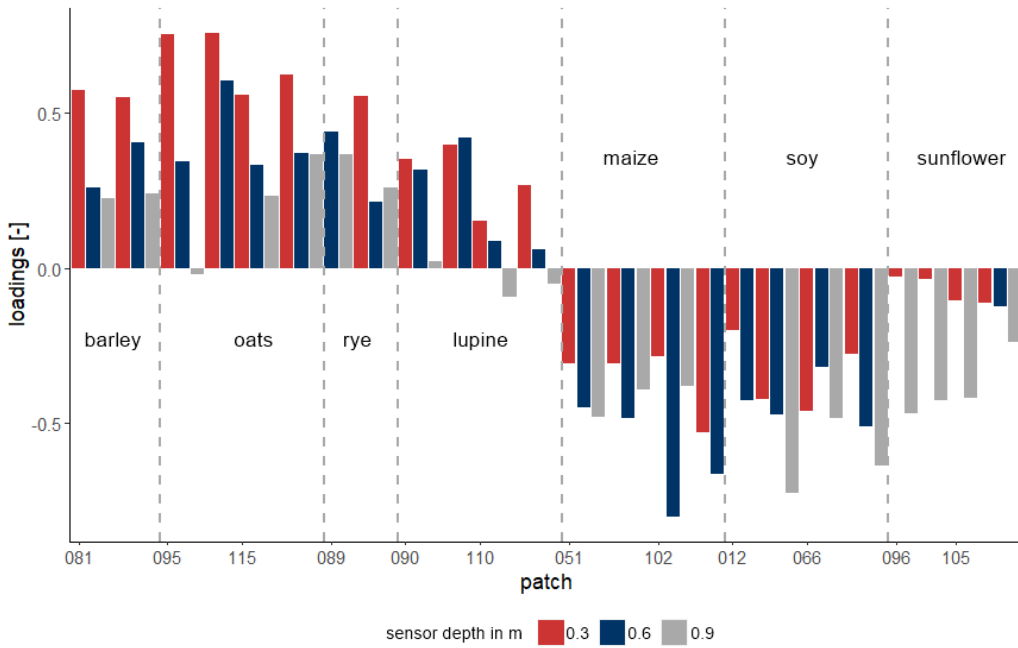
598

599 **Figure 2: Input soil moisture time series per depth, differentiated between crop groups, and average soil moisture of all time series**  
 600 **per depth from 2020-12-01 until 2021-08-15 at the patchCROP landscape laboratory, Tempelberg, Brandenburg, Germany.**



601

602 **Figure 3: Measured daily precipitation, mean temperature and cultivated crops - differentiated between winter crops (light blue**  
 603 **bars), summer crops (green bars) and cover crops (pink bars) - from 2020-12-01 until 2021-08-15 at the patchCROP landscape**  
 604 **laboratory, Tempelberg, Brandenburg, Germany. Specific crops for the studied timeframe stated at the left side of the horizontal**  
 605 **bars.**



606

607 **Figure 4: Time series loadings on the second principal component at the patchCROP landscape laboratory, Tempelberg,**  
 608 **Brandenburg, Germany, showing a crop group related pattern. Bars represent individual time series grouped by patch ID and**  
 609 **sorted by crop.**

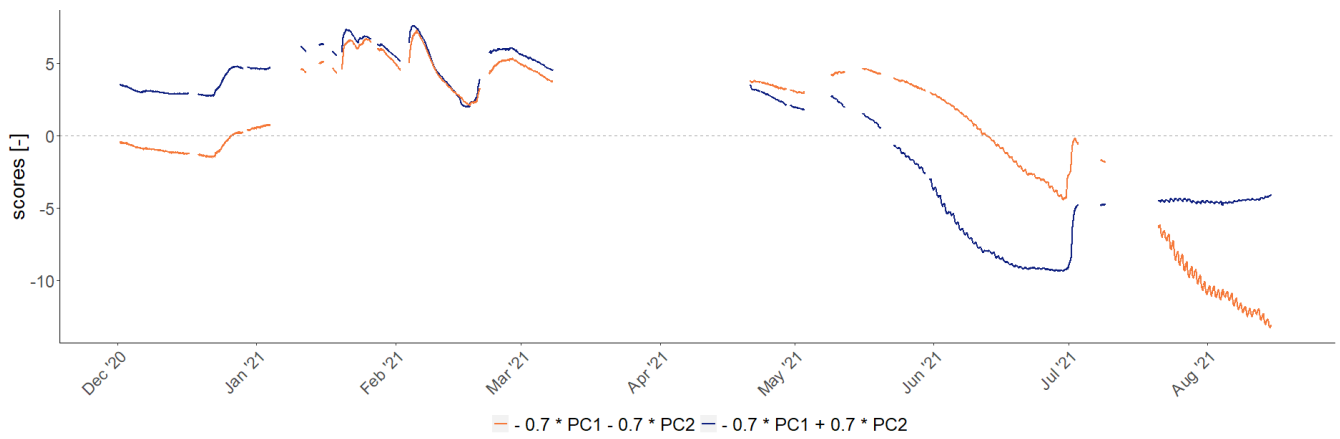


**Figure 5: Effect of the second principal component on modification of the general mean behaviour presented by the first principal component at the patchCROP landscape laboratory, Tempelberg. The blue line represents deviations from mean soil moisture for time series with positive loadings on PC2 (winter crops) while the orange line represents deviations from mean soil moisture for time series with negative loadings on PC2 (summer crops).**

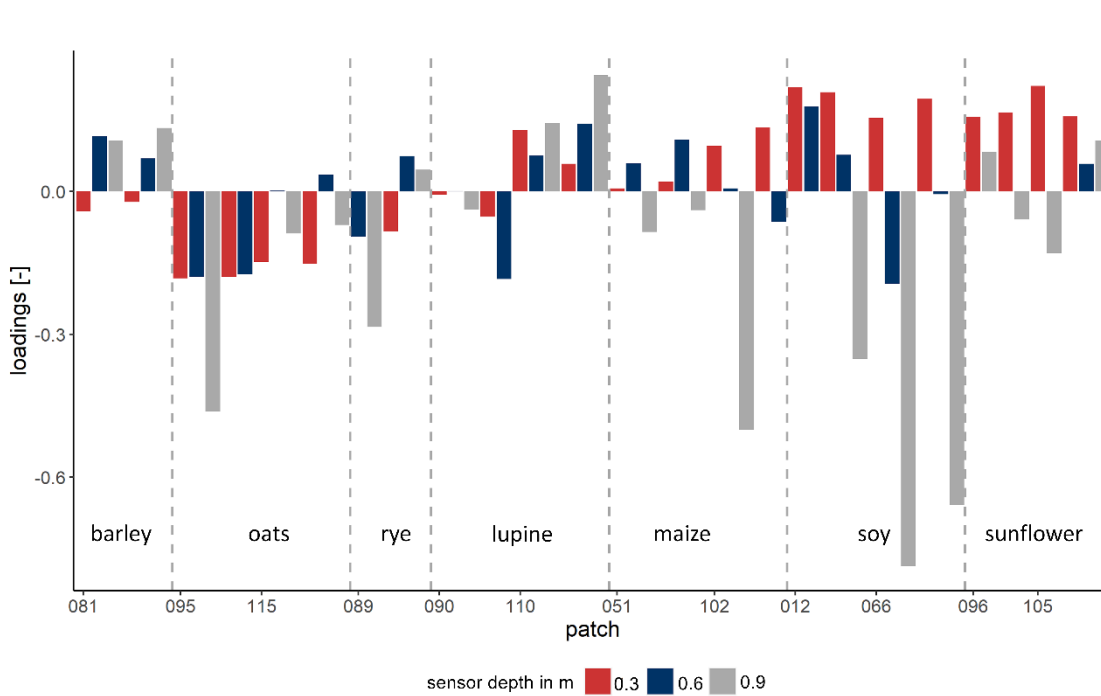
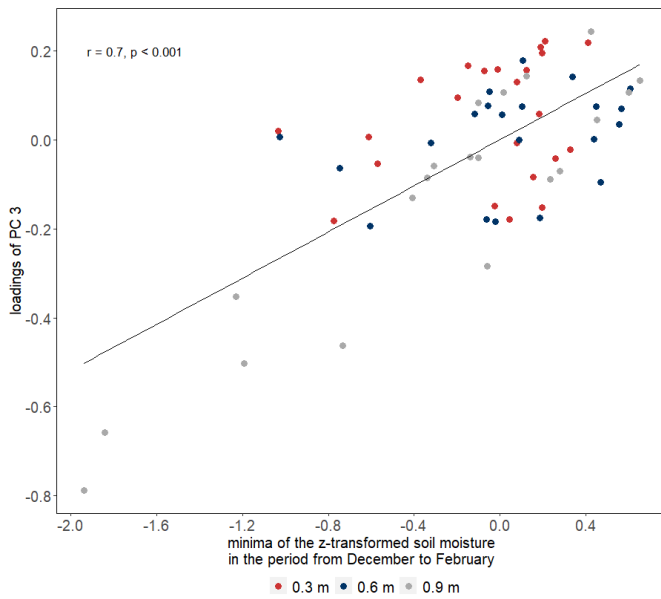


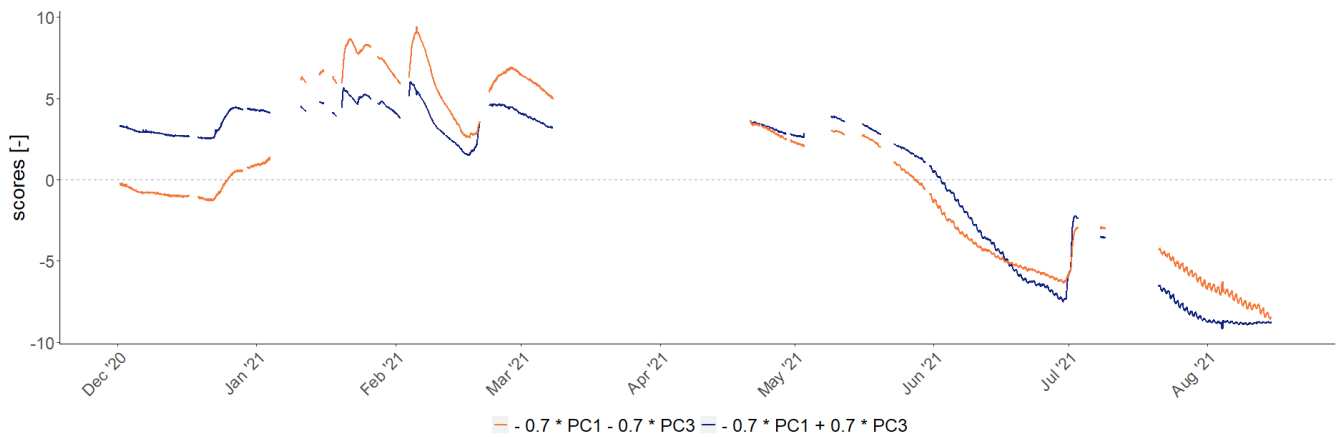
**Figure 6: Loadings of time series on the third principal component at the patchCROP landscape laboratory, Tempelberg, Brandenburg, Germany with some of the sensors in deeper layers showing noticeably negative loadings. Bars represent individual time series grouped by patch ID and sorted by crop.**



620

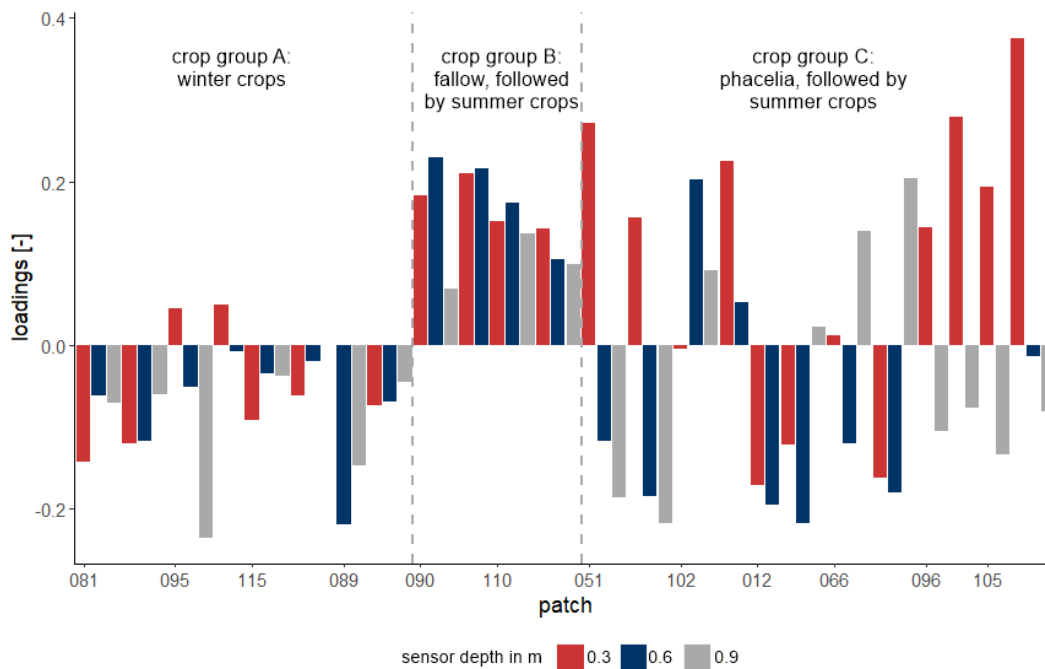
621 **Figure 7: Relation between minima of the z-transformed soil moisture in the first months of the study period with loadings of third**  
 622 **principal component showing that sensors with noticeably negative loadings showed distinctly negative z-transformed minima.**

623



624

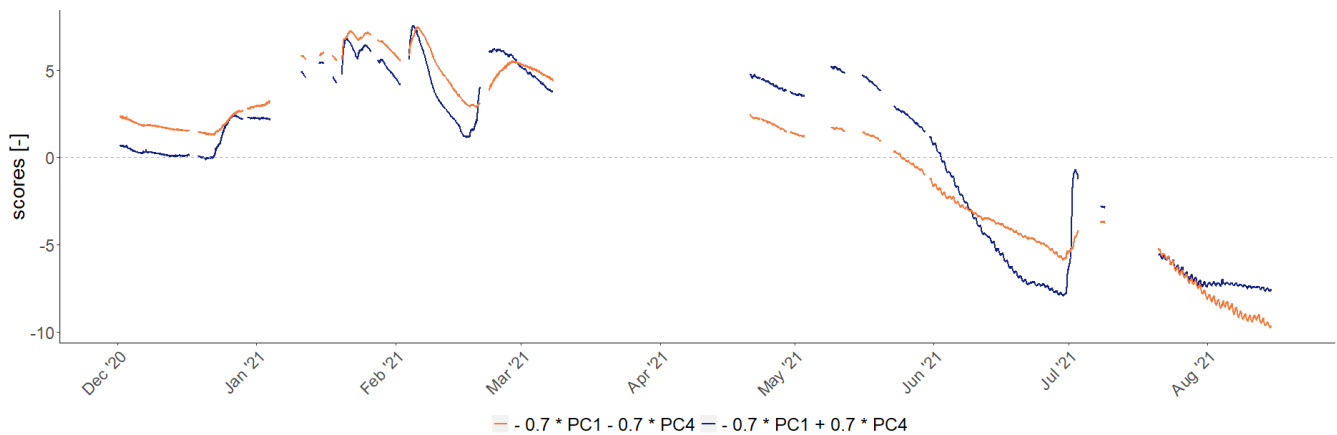
625 **Figure 8: Effect of the third principal component on modification of the general mean behaviour presented by the first principal**  
 626 **component at the patchCROP landscape laboratory, Tempelberg. The blue line represents deviations from mean soil moisture for**  
 627 **time series with positive loadings on PC3 (majority of the time series) while the orange line represents deviations from mean soil**  
 628 **moisture for time series with negative loadings on PC3 (part of the sensors in 0.9 m depth).**



630

631 **Figure 9: Loadings of time series on the fourth principal component at the patchCROP landscape laboratory, Tempelberg,**  
 632 **Brandenburg, Germany showing mainly negative loadings for crop group A, positive loadings for crop group B and loadings with**  
 633 **no clear pattern for crop group C. Bars represent individual time series grouped by patch ID, sorted by treatment group.**

634

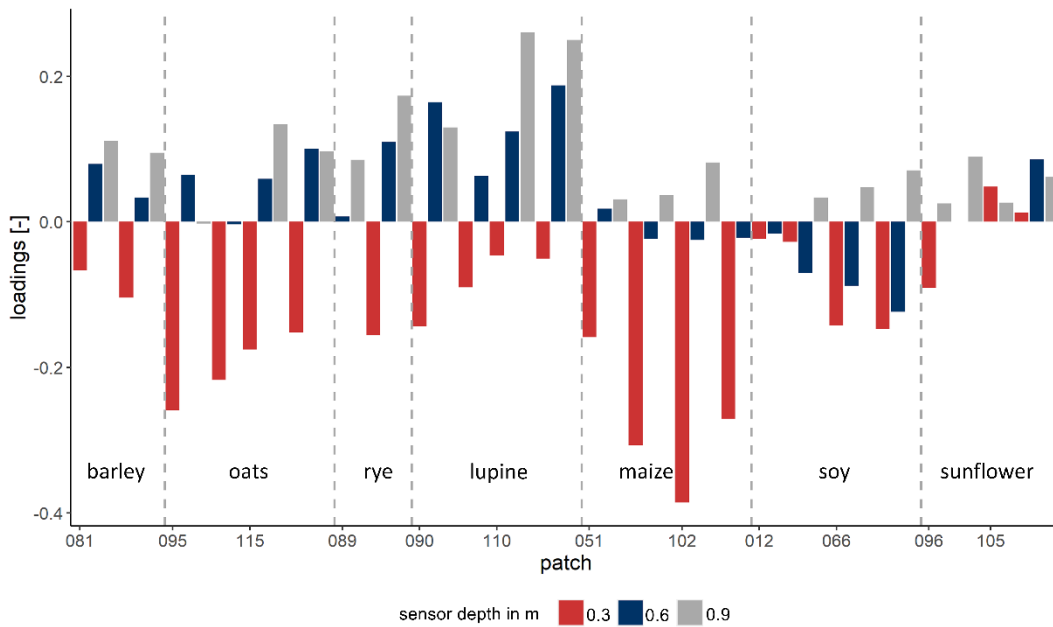


635

636 **Figure 10: Effect of the fourth principal component on modification of the general mean behaviour presented by the first principal**  
 637 **component at the patchCROP landscape laboratory, Tempelberg. The blue line represents deviations from mean soil moisture for**  
 638 **time series with positive loadings on PC4 (single sensors of crop group A, all sensors of crop group B, and part of crop group C)**  
 639 **while the orange line represents deviations from mean soil moisture for time series with negative loadings on PC4 (most sensors of**  
 640 **crop group A and part of the sensors of crop group C).**



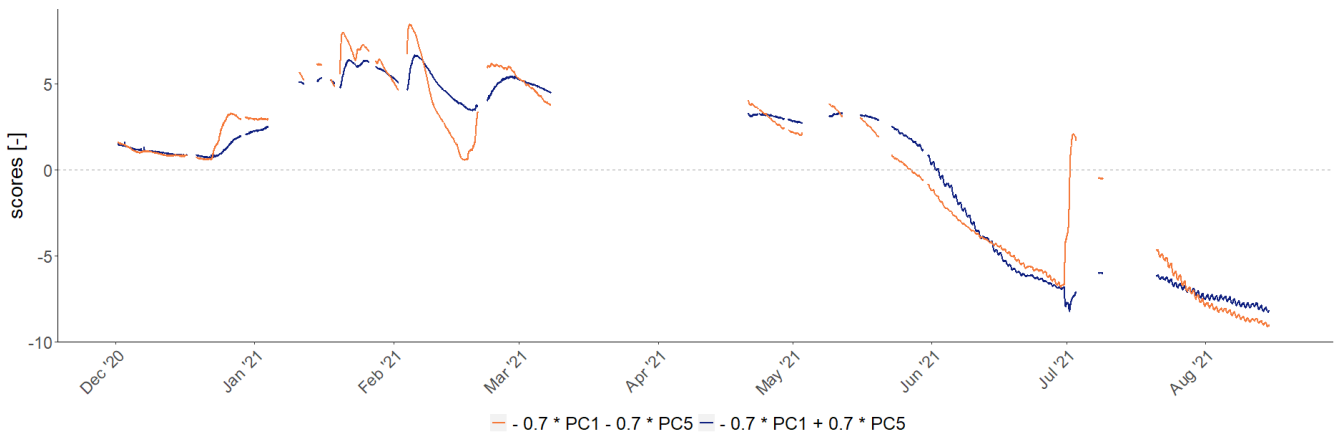
641



642

643 **Figure 11: Loadings of time series on the fifth principal component at the patchCROP landscape laboratory showing a depth**  
644 **related pattern. Bars represent individual time series grouped by patch ID, sorted by crop.**

645



646

647 **Figure 12: Effect of the fifth principal component on modification of the general mean behaviour presented by the first principal**  
648 **component at the patchCROP landscape laboratory, Tempelberg. The blue line represents deviations from mean soil moisture for**  
649 **time series with positive loadings on PC5 (sensors in greater depth) while the orange line represents deviations from mean soil**  
650 **moisture for time series with negative loadings on PC5 (sensors in shallow depth).**

651 **Table 1: Overview of crop rotation, sand content in the top 0.25 m soil depth and weed control for selected patches at the patchCROP**  
 652 **landscape laboratory, Tempelberg, Brandenburg, Germany.**

Crop in winter season	Crop in summer season	Crop group	Sand content (in 1 m buffer zone around sensors) in %	Weed control	Patch ID
Winter barley		A	78.3	conventional	81
Winter oats		A	80.7	conventional	95
Winter oats		A	80.6	reduced	115
Winter rye		A	80.5	conventional	89
Fallow	Lupine	B	80.6	conventional	90
Fallow	Lupine	B	80.3	reduced	110
Phacelia	Maize	C	80.8	reduced	51
Phacelia	Maize	C	80.6	conventional	102
Phacelia	Soy	C	78.5	reduced	12
Phacelia	Soy	C	77.9	conventional	66
Phacelia	Sunflower	C	80.6	conventional	96
Phacelia	Sunflower	C	80.5	reduced	105

653

654 **Table 2: Overview of normalized difference vegetation index (NDVI), surface temperature, and slope at the locations of analysed**  
 655 **sensors at the patchCROP experiment in Tempelberg, Brandenburg, Germany.**

Crop	Patch ID	Sensor Position	NDVI 2021-05-20 [-]	NDVI 2021-05-31 [-]	NDVI 2021-07-06 [-]	Surface Temperature 2021-05-31 in °C	Slope in °
Winter barley	81	West	0.874	0.182	0.926	20.57	2.01
Winter barley	81	East	0.875	0.180	0.927	20.43	1.94
Winter oats	95	East	0.838	0.208	0.834	27.25	1.36
Winter oats	95	West	0.838	0.213	0.840	27.85	1.15
Winter oats	115	West	0.756	0.278	0.845	23.70	1.28
Winter oats	115	East	0.783	0.281	0.863	25.12	0.43
Winter rye	89	West	0.796	0.263	0.856	22.39	1.74
Winter rye	89	East	0.787	0.206	0.822	24.95	1.67
Lupine	90	West	0.185	0.395	0.710	26.31	1.40
Lupine	90	East	0.203	0.391	0.733	24.96	1.27
Lupine	110	West	0.090	0.563	0.635	26.98	1.88
Lupine	110	East	0.090	0.567	0.639	26.76	2.50

Maize	51	West	-0.099	0.654	0.181	35.44	0.82
Maize	51	East	-0.096	0.638	0.217	35.29	0.93
Maize	102	West	-0.077	0.714	0.175	37.88	0.88
Maize	102	East	-0.058	0.728	0.178	38.03	0.90
Soy	12	West	-0.107	0.748	0.166	34.87	1.71
Soy	12	East	-0.108	0.723	0.162	34.44	1.11
Soy	66	West	-0.115	0.730	0.144	35.09	2.40
Soy	66	East	-0.114	0.661	0.147	34.39	2.13
Sunflower	96	West	-0.109	0.816	0.211	33.76	0.59
Sunflower	96	East	-0.101	0.827	0.229	34.70	0.69
Sunflower	105	West	0.178	0.610	0.564	29.79	1.04
Sunflower	105	East	0.030	0.696	0.399	34.53	1.00

656

657 **Table 3: Statistical characteristics and interpretations of principal components 1 to 5 for soil moisture dynamics of selected patches**  
658 **at the patchCROP landscape laboratory, Tempelberg, Brandenburg, Germany.**

	<b>PC1</b>	<b>PC2</b>	<b>PC3</b>	<b>PC4</b>	<b>PC5</b>
<b>Eigenvalue</b>	46.25	10.89	2.60	1.43	1.06
<b>Proportion of variance in %</b>	72.27	17.01	4.06	2.23	1.65
<b>Proportion of variance (cumulative) in %</b>	72.27	89.28	93.34	95.57	97.22
<b>Interpretation</b>	Mean behaviour	Winter vs. summer crops	Subsoil texture	winter vegetation cover and influence of cover crops on soil	Damping of the input signal
<b>Prevailing driver</b>	weather	crop	soil	crop and soil	soil

659

660 **Table 4: Pearson correlation coefficients between surface temperature and normalized difference vegetation index (NDVI) at the**  
661 **patchCROP landscape laboratory, Tempelberg, Brandenburg, Germany, and loadings of sensors in all depths or at single depths,**  
662 **respectively, on the second principal component. All correlations were highly significant ( $p < 0.01$ ).**

<b>Variable</b>	<b>Sensors in all depths</b>	<b>0.3 m</b>	<b>0.6 m</b>	<b>0.9 m</b>
<b>Surface temperature</b>	-0.853	-0.881	-0.909	-0.916
<b>NDVI 2021-05-20</b>	0.836	0.904	0.837	0.907
<b>NDVI 2021-05-31</b>	0.899	0.945	0.944	0.946

NDVI 2021-07-06

-0.860

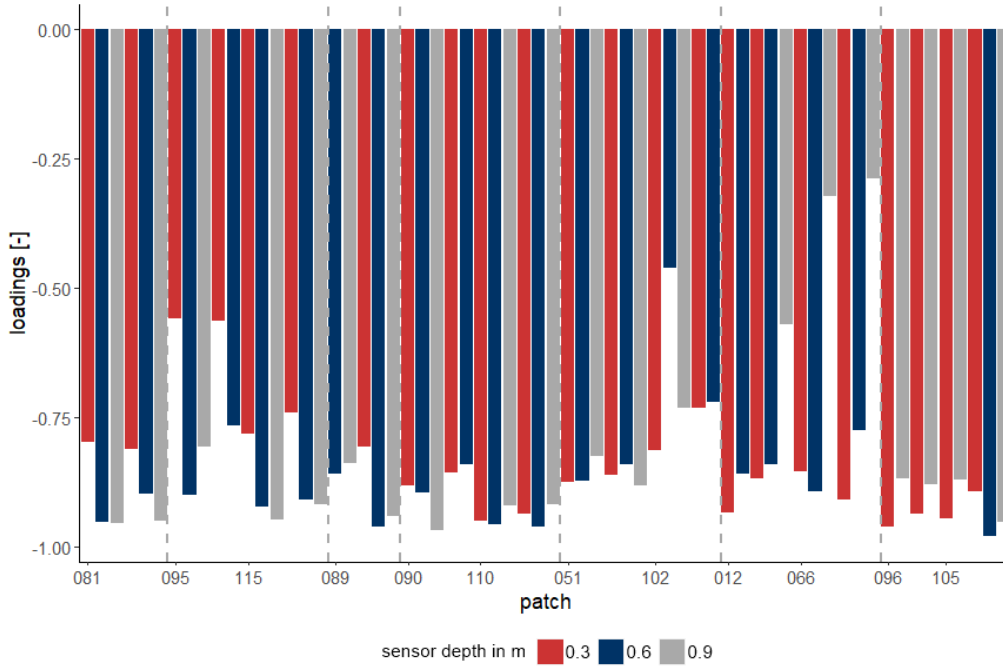
-0.898

-0.917

-0.913

663

664 APPENDIX A



665

666 **Figure 13: Loadings of time series on the first principal component at the patchCROP landscape laboratory, Tempelberg,**  
667 **Brandenburg, Germany. Bars represent individual time series grouped by patch ID and sorted by crop.**